# NOVEL INFRARED SENSORS USING MICRO- AND NANO-ELECTROMAGNETIC METAMATERIALS

B. D. F. CASSE, H. O. MOSER†, M. BAHOU, B. T. SAW, L. K. JIAN and P. D. GU
*Singapore Synchrotron Light Source (SSLS), National University of Singapore (NUS), 5 Research Link, Singapore 117603*
†*E-mail: moser@nus.edu.sg*

O. WILHELMI
*FEI Electron Optics BV, Achtseweg Noord 5, 5621 GG Eindhoven, The Netherlands*

The fabrication of micro- and nanoElectroMagnetic MetaMaterials ($EM^3$) and their potential application in novel infrared sensors are reported. $EM^3$ refers to composite materials having both, permittivity and permeability, negative simultaneously which leads to a plethora of unusual effects such as a negative index of refraction and an inverse Doppler and Čerenkov effect. The gold-plated micro composites, based on a rod-split-ring-resonator design are arranged in an array and embedded in a $2 \times 2$ mm$^2$ plastic chip, while the nano composites also made out of gold stand freely on a 0.5-mm thick glass substrate. Numerical simulations and experimental results from the ISMI (Infrared Spectro/MIcroscopy) facility at SSLS show that the composite materials which have feature sizes down to 50 nm are $EM^3$ in the range 1–193 THz (FIR–NIR). Transmission experiments demonstrate that the rod-split-ring-resonator possesses band-pass filter characteristics on resonance. Depending on design, this band-pass can be shifted to a specific frequency range or converted to a stop band by slight alteration of the geometric dimensions, or structure, of the composite materials, making such filters attractive for novel light-weight infrared (IR) sensors.

## 1 Introduction

During the last few years, there has been a significant effort, in particular in the U.S., for advancing THz-frequency electronic technology and developing novel applications of THz-frequency sensing [1]. Driving forces behind the research into THz technologies include ideas of building high-frequency wireless systems for satellites and military applications as well as sensing and characterizing chemical and biological (CB) agents. Practically all terahertz sensing devices (or IR sensors) need optical filters to optimize their performance. Band-pass filters are used for separation of spectral bands over a wide spectral region in order to increase the signal-to-noise (S/N) ratio for a specific region. Such filters nowadays have demonstrated remarkable performance capabilities, but suffer from high cost, poor manufacturing yield, excessive weight and are prone to degradation under the presence of dust and scratches [2].

In this paper, we address the fabrication of micro- and nanofabricated electromagnetic metamaterials suitable for new arbitrary frequency band-pass filters operating from the far infrared up to telecommunications frequencies. Produced by established LIGA [3] techniques, such filters would represent a low-cost, light-weight and robust option for integration into IR sensors. One of the most critical applications of such a filter is to block unwanted radiation from nearby military high-power laser, while still allowing the sensor to conduct necessary battlefield operations.

Metamaterials, in general, refer to composite materials which feature electromagnetic properties usually not found in nature, from their structure rather than from the intrinsic properties of constituent materials. V. G. Veselago, in his pioneering paper in 1967 [4], made a systematic theoretical study of electromagnetic properties of hypothetical materials having simultaneously negative permittivity $\epsilon$ and permeability $\mu$. These materials, which he termed as "*left-handed materials*", would exhibit a myriad of interesting properties such as a negative index of refraction and an inverse Doppler and Čerenkov effect. The unavailability of left-handed materials in nature plunged Veselago's work into slumber for thirty years. In the 1990s, Sir John Pendry and coworkers revived the interest in Veselago's work by looking into theoretical models for obtaining $\epsilon_{\text{eff}} < 0$ [5] and $\mu_{\text{eff}} < 0$ [6] by a combination of wire arrays and split-ring resonators (SRRs). Pendry's inspiring work led to a resurgence of effort in fabricating electromagnetic metamaterials with first demonstrations in the GHz range [7].

Since 2003, we applied lithography to the manufacturing of the next generation $EM^3$, thus producing the first microelectromagnetic metamaterials in the far infrared region [8]. Continuing these efforts towards nanofabrication [9] [10], we were able to produce electromagnetic metamaterials operating at a record frequency of ∼187.5 THz [11], which is close to telecommunications frequencies.

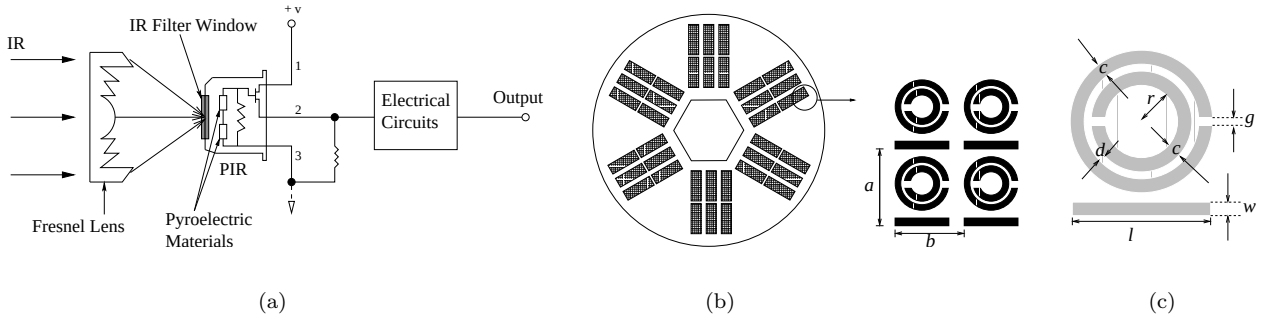


(a) (b) (c)

Figure 1. (a) Typical configuration of an infrared sensor device (modified after [12]). (b) "*Shutter wheel*" filter window design with EM$^3$ rod-split-ring arrays. (c) The planar adaptation of Pendry-Smith prototype for 2D micro/nanofabrication. Geometric parameter definition of unit cells.

## 2 Selectable Wavelength Filter Design in Infrared Sensor Devices

Figure 1(a) shows the typical configuration of an IR sensor device. The heart of the device is the Passive Infrared (PIR) sensor, which comprises a filter window and pyroelectric materials. We envisage the filter window in the form of a "*shutter wheel*" as shown in figure 1(b). The wheel consists of several windows, each of them containing arrays of rod-split-ring (RSR) resonators, with different geometric parameters which would correspond to specific resonance frequencies. The arrays can be manufactured using batch processing X-ray lithography, and later on by hot embossing, to speed up production rate. The geometric parameter definition of the RSR and the periodic arrangement adopted for microfabrication is shown in figure 1(c). In this system, the rods have a negative permittivity just below their plasma frequencies, $\omega_p$ as described by the Drude model [13]. The split ring resonator (SRR) can be viewed as an LC circuit [6] with a dispersive effective permeability. While the usable bandwidth for which $\epsilon_{\text{eff}} < 0$ is much larger than that of $\mu_{\text{eff}} < 0$, provided that a small ratio of radius to distance of the wires is used, the lower and upper limit of the frequency interval over which $\mu_{\text{eff}} < 0$ was calculated from Pendry's analytical formula [6]

$$\nu_0 = \frac{1}{2\pi}\sqrt{\frac{3dc_0^2}{\pi^2 r^3}} < \nu_{\text{mp}} = \frac{\nu_0}{\sqrt{1-\pi r^2/ab}} \qquad (1)$$

where $c_0$ is the speed of light *in vacuo*. Five and four geometric variants were used for the micro- and nanofabrication of EM$^3$, respectively. The sets of those geometric parameters and the limits of the interval in which the composites have EM$^3$ behavior are shown in references [8 9 10 11].

## 3 Micro- and Nanofabrication of Electromagnetic Metamaterials

The pattern of the microelectromagnetic metamaterials process were directly written by laser beam on the AZ P4620 photoresist. Subsequent development of the resist and electroforming generated the metal structures embedded in the resist matrix. Released from the silicon substrate by etching the chromium sacrificial layer in between resist and substrate, the final products are 2 × 2 mm$^2$ microchips consisting of nickel or gold RSRs held in the AZ P4620 plastic matrix as shown in figure 2 (a). More process details of the microtechnology process were outlined in references [8 9].

The pattern of the nanoelectromagnetic metamaterials were written by a 30 keV electron beam into PMMA resist spin-coated on top of either a glass or a silicon substrate. In these cases, the substrate is transparent within the relevant spectral range and therefore release of the metal-filled matrix is not necessary. The voids created by the development are then filled with metal via magnetron sputtering. A final lift-off of the PMMA resist was achieved by immersing the sample in acetone for 1 hour. The end product is a 500 × 500 µm$^2$ array of 30 nm thick gold RSR on 0.5 mm thick glass substrate as shown in figure 2 (b). More details of the nanofabrication processes may be found in references [9 10 11]. The fabrication techniques described above were used initially for rapid prototyping and characterization of the composite materials. To manufacture EM$^3$ in bulk quantities for the marketplace, we have to resort to the full LIGA process.

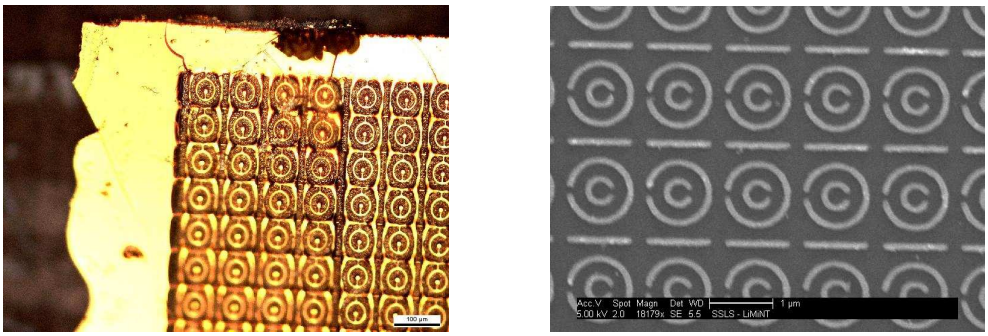

(a) (b)

Figure 2. (a) 2 × 2 mm$^2$ gold RSRs microchips embedded in the AZ P4620 plastic matrix (scale bar 100 µm). (b) 500 × 500 µm$^2$ of 30 nm thick gold RSRs on 0.5-mm thick free-standing glass substrate (scale bar 1 µm).

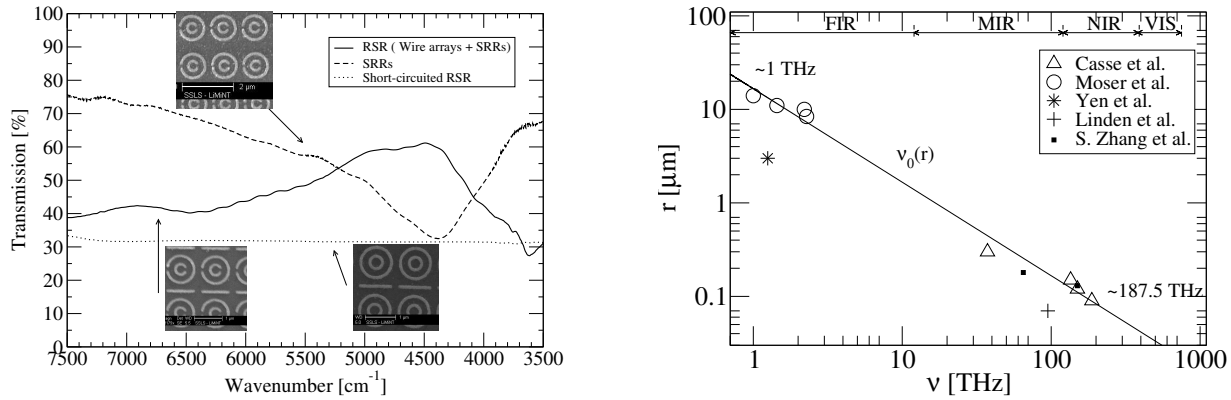


(a) (b)

Figure 3. (a) Typical transmission spectra of SRR and RSR and short-circuited RSR. (b) Plot of radius $r$ of the SRR versus frequency over the spectral range from 1 THz to 1 PHz.

## 4 Characterization and Optimization of Electromagnetic Metamaterials

For the microstructures, the spectroscopic measurements (in transmission mode) were performed using a Bruker IFS 66 v/S Fourier transform interferometer, at the Infrared Spectro-MIcroscopy beamline (ISMI), in the far infrared (FIR) over the range of 22 to 400 cm$^{-1}$ with a 4 cm$^{-1}$ and 2 cm$^{-1}$ spectral resolution. The microchips were mounted in the FTIR at normal incidence to the unpolarized beam. Axial magnetic field components needed to induce the current in the split rings are due to the angular spread of the beam and diffraction at the surface.

Transmission experiments on the nanoEM$^3$ composites were performed with Bruker's Hyperion 2000 Microscope at the ISMI beamline. The Hyperion microscope was set to reflection-transmission mode for the experiment with a first transmission through the sample, followed by a reflection on a silver mirror and a second transmission through the sample before reaching the detector. The mean incidence angle of the beam on the samples was 23° to the normal, as set by the Schwarzschild objective. Both the micro- and nano-RSR samples showed characteristics of a bandpass filter in the relevant spectral region. As a further evidence of EM$^3$ behavior, a composite material was fabricated with the azimuthal gap $g$ of the split rings closed, the short-circuited sample, thus destroying the magnetic resonance of the SRR [14]. The closed ring structure did not show any electromagnetic response in the relevant frequency range as expected.

A typical EM$^3$ spectrum and associated SRR/short-circuited RSR is given in figure 3(a). For the case of the SRR, we can observe an attenuation in transmission (or stop band) between 4000 and 5000

$cm^{-1}$ in the curve of the SRR alone, which corresponds to the region of negative $\mu_{\text{eff}}$. Now combining the SRRs with the wire arrays (RSRs), a band-pass emerges (characterized by an increase in transmission) around the same frequency range indicating that both $\epsilon_{\text{eff}}$ and $\mu_{\text{eff}}$ are negative. No prominent peaks are observed in the case of the short-circuited RSRs. Figure 3(b) shows the plot of inner radius versus frequency for split ring resonators over the spectral range from 1 THz to 1 PHz. $\nu_0(r)$ is Pendry's analytical formula introduced in equation (1). The open symbols mark results measured by the present authors while the symbols $(*)$ and $(+)$ denote results obtained by Yen *et al.* ($\sim$1.25 THz) [15] and Linden *et al.* ($\sim$100 THz)[16], respectively. The symbol (■) denotes resonance frequencies of $\sim$65 THz [17] and $\sim$150 THz [18] obtained by S. Zhang *et al.* The straight line is Pendry's formula for the resonance frequency of a circular nested SRR. The experimental results are in good agreement with both Pendry's analytical formula and numerical simulations (not shown in this paper).

From equation (1), we observe that the resonant frequency scales as $d^{0.5}\ r^{1.5}$. Hence to shift the band-pass or resonant frequency either the inner radius $r$ or the inter-ring distance $d$ could be varied, while keeping other geometric parameters constant. Weiland *et al.* [19] predict a weak dependence of the resonant frequency on the azimuthal gap ($g^{0.08}$) and the thickness ($t^{-0.09}$) of the ring. Chevalier and Wilson [20] have calculated the influence of the various geometric parameters on the bandwidth. Hence the bandwidth of the pass-band can be altered by optimizing the various geometric parameters and lattice constant.

## 5 Conclusion

We have fabricated a new class of micro- and nano-materials, so-called electromagnetic metamaterials, with overall structure size below 100 µm (structural details down to 5 µm) and 1 µm (structural details down to 50 nm), respectively. Furthermore we have addressed the integration of such electromagnetic metamaterials as band-pass filters in sensor devices to optimize the latter. The pass-bands can be set to specific frequency ranges and their bandwidth can also be altered simply by fine-tuning the geometric dimensions of the composite materials. The end results are low-cost, light-weight, band-pass/stop-band filters in IR sensor devices. These novel infrared sensors have a wide variety of applications ranging from space-based systems to military applications.

**Acknowledgments**

The authors would like to thank Lim Hock and Gan Yeow Beng from the Temasek Laboratories, NUS, for valuable discussions. Work performed at the Singapore Synchrotron Light Source (SSLS) under A*STAR/MOE RP3979908M, A*STAR 0121050038, and NUS Core Support C-380-003-003-001 grants.

## References

1. Defense Advanced Research Project Agency (DARPA) program on "Terahertz Technology for Sensing and Satellite Communications" and a Multidisciplinary University Research Initiative (MURI) program on "Sensing Science and Electronic Technology at THz Frequencies".
2. A. R. Jha. *Infrared Technology: Applications to electro-optics, photonic devices, and sensors.* John Wiley & Sons, 2000.
3. E. W. Becker, W. Ehrfeld, D. Munchmeyer, H. Betz, A. Heuberger, S. Pongratz, W. Glashauser, H. J. Michel, and V. R. Siemens. *Naturwissenschaften*, 69:520–523, 1982.
4. V. G. Veselago. *Sov. Phys. Usp.*, 10:509, 1968.
5. J. B. Pendry, A. J. Holden, W. J. Stewart, and I. Youngs. *Phys. Rev. Lett.*, 76:4773, 1996.
6. J. B. Pendry, A. J. Holden, D. J. Robbins, and W. J. Stewart. *IEEE Trans. Microwave Theory Tech.*, 47:2075, 1999.
7. D. R. Smith, Willie J. Padilla, D. C. Vier, S. C. Nemat-Nasser, and S. Schultz. *Phys. Rev. Lett.*, 84:4184, 2000.
8. H. O. Moser, B. D. F. Casse, O. Wilhelmi, and B. T. Saw. *Phys. Rev. Lett.*, 94(6):063901, 2005.
9. B. D. F. Casse, H. O. Moser, O. Wilhelmi, and B. T. Saw. *Micro- and Nano-Fabrication of Electromagnetic Metamaterials for the Terahertz range,* Proceedings of the ICMAT 2005 Symposium R. pages 18–25, Singapore, 2005. World Scientific.
10. H. O. Moser, B. D. F. Casse, O. Wilhelmi, and B. T. Saw. *Electromagnetic Metamaterials over the whole THz range — achievements and perspectives*, Proceedings of the ICMAT 2005 Symposium R. pages 55–58, Singapore, 2005. World Scientific.
11. B. D. F. Casse, H. O. Moser, M. Bahou, L. K. Jian, and P. D. Gu. *in press for IEEE Transactions on Nanotechnology*, 2006.
12. http://www.glolab.com
13. D. Pines and D. Bohm. *Phys. Rev.*, 85:338, 1952.
14. K. Aydin, K. Guven, M. Kafesaki, L. Zhang, C. M. Soukoulis, and E. Ozbay. *Opt. Lett.*, 29(22):2623–2625, 2004.
15. T. J. Yen, W. J. Padilla, N. Fang, D. C. Vier, D. R. Smith, J. B. Pendry, D. N. Basov, and X. Zhang. *Science*, 303:1494, 2004.
16. Stefan Linden, Christian Enkrich, Martin Wegener, Jianfeng Zhou, Thomas Koschny, and Costas M. Soukoulis. *Science*, 306:1351, 2004.
17. S. Zhang, W. Fan, B. K. Minhas, A. Frauenglass, K. J. Malloy, and S. R. J. Brueck. *Phys. Rev. Lett.*, 94:37402, 2005.
18. Shuang Zhang, Wenjun Fan, N. C. Panoiu, K. J. Malloy, R. M. Osgood, and S. R. J. Brueck. *Phys. Rev. Lett.*, 95:137404, 2005.
19. T. Weiland, R. Schuhmann, R. B. Greegor, C.G. Parazzoli, and A. M. Vetter. *J. Appl. Phys.*, 90:5419, 2001.
20. Christine T. Chevalier and Jeffrey D. Wilson. Technical Report NASA/TM—2004-213403, National Aeronautics and Space Administration (NASA), 2004.